Science
AAAS

Supplementary Materials for

Brain activity of diving seals reveals short sleep cycles at depth

Jessica M. Kendall-Bar *et al*.

Corresponding author: Jessica M. Kendall-Bar, jkb@ucsc.edu

Science **380**, 260 (2023)
DOI: 10.1126/science.adf0566

The PDF file includes:

Other Supplementary Material for this manuscript includes the following:

Materials and Methods

Procedures & Ethics Statement

All animal procedures were approved at the federal and institutional levels under National Marine Fisheries Permits 496, 836, 786–1463, 87-1743, 19108, 14636, and 23188, and by the Institutional Animal Care and Use Committee (IACUC) of University of California Santa Cruz (Costd1709 and Costd2009-2). All animals were sedated for tag placement following standard protocols (*15, 18, 23, 35-40*). Briefly, an induction injection of intramuscular Telazol® [tiletamine and zolazepam] (1 mg/kg) was maintained with doses of Telazol/ketamine/valium as needed. With the exception of the EEG headcap and patches which were attached with flexible, skin-compliant AquaSeal™ (GEAR AID ®), all other tags were attached via flexible nylon mesh epoxied to the animal's fur, consistent with established practices for external attachment of animal telemetry tags (*41*). At each handling, most animals were weighed in a canvas sling from a hanging scale with precision ±1 kg.

Animals and Instrumentation

(1) Sleep (EEG) Recordings.

We recorded electroencephalogram (EEG), electrocardiogram (ECG), electrooculogram (EOG), electromyogram (EMG), depth, environmental temperature, illumination, and three-dimensional inertial motion sensing (accelerometry, magnetometry, and gyroscope) in 13 juvenile female northern elephant seals using a custom, non-invasive EEG headcap and ruggedized housing ((*18*); Table S1). The custom headcap attached with AquaSeal™ adhesive (GEAR AID ®) was designed to minimize water intrusion to surface-mounted Genuine grass goldcup electrodes measuring the front-parietal derivations of the left and right hemisphere (4 EEG, 2 EOG signals). Patches attached near the pectoral flippers and neck measured ECG and EMG. The custom, ruggedized, and waterproofed (>2000 m) housing contained a Neurologger3 (© 2016 Evolocus LLC) for data storage at 500Hz (electrophysiological signals) and ~36Hz (250/7 ≈ 35.7143Hz; environmental and motion sensors) on a 200 GB microSD card. We down-sampled inertial motion sensors to 8 s intervals for the training and validation of the sleep-identification model of a larger dataset, including records with 8 s intervals. Details of the instrument development have been reported in Kendall-Bar *et al.* 2022 (*18*).

(1A) Sleep in the lab. First, we recorded sleep in 5 juveniles (2 8-month-olds and 3 20-month-olds) temporarily housed at Long Marine Lab at UC Santa Cruz in Santa Cruz, CA on land (310.4 h total – 12.6 days) and in a shallow pool (4.9 m x 3.0 m x 1.4 m; 153.5 h total – 6.3 days). ***(1B) Sleep in the wild.*** Next, we instrumented 6 seals (3 2-month-olds and 3 juveniles [14 or 24 months old]) on the beach that stayed on land (375.9 h total – 14.3 days) and in shallow lagoons (205.5 h total – 8.3 days) at Año Nuevo State Park, CA. One of these seals also carried an animal-borne camera. ***(1C) Sleep at sea.*** We recorded sleep at sea from 3 seals (3 juveniles [~24 months old]; 194.4 h total – 8.1 days at sea). One was instrumented on the beach and spent 43.9 h at sea before returning to the beach. The other two seals were translocated ~60 kilometers south of Año Nuevo State Park and released at Asilomar Beach in Monterey, CA. For all seals, instruments were recovered 2.5-5 days after attachment (total of 51.6 recording days). Recordings of EEG in juveniles at sea (8.1 days total) were used to determine quantitative thresholds to interpret and identify behavioral sleep in the following categories: time-depth and stroke-rate recordings in adult females. The translocation-homing paradigm with juvenile seals

facilitates short-term collection of high-resolution data from juvenile seals whose diving behavior is similar to migrating adult seals *(35, 36)*. Seals are translocated to an area that requires them to cross the deep Monterey canyon, similar to the deep and pelagic waters of the adult females' range.

(2) Time-depth Recorder (TDR) Recordings.

Between 2004 and 2019, we instrumented 334 adult (>3 years old) female northern elephant seals with time-depth recorders and satellite transmitters (multiple models produced by Wildlife Computers, Redmond, WA, USA or Sea Mammal Research Unit, St Andrews, UK) for their post-molt or post-breeding foraging trips according to established protocols (3*7*–3*9*) (Table S1). Data was collected at 4 or 8 s intervals. We down-sampled 4 s interval data to 8 s intervals for consistency.

(3) Stroke-Rate (SR) Recordings – Validation subset.

A subset of these TDR seals was instrumented with accelerometers (N=14). Accelerometers allowed detection of individual swimming strokes (using back- or flipper-attached accelerometers) and foraging attempts (from jaw-attached accelerometers). We used these recordings to calculate the false positive rate for our sleep identification model (see 'Sleep Identification Validation' below). Original data was processed onboard from 32Hz accelerometer data into 5 s bins using customized "kami kami" dataloggers (Little Leonardo, Tokyo, Japan; *17*, *39*). We down-sampled the data 10 s intervals, and subsequently paired to the KNN-nearest-neighbor 8 s sample to maintain consistency across the larger dataset (sampled at 8 s). We defined glides as consecutive segments where stroke rate was less than 15 strokes per minute. This threshold allowed elimination of short-duration peaks up to 15 strokes per minute that were likely associated with passive postural movements rather than swimming propulsion (active stroking was between 40-70 strokes per minute).

<u>EEG: Purpose & Justification</u>

Sleep in marine mammals and birds is unique given that inactivity matching the definition of behavioral sleep can be entirely absent (*10, 11*). As a result, electrophysiological recordings are essential to assess total sleep time. EEG recordings also discriminate rapid eye movement (REM) from non-REM slow-wave sleep (SWS), each with physiological and behavioral implications. Most notably for an animal sleeping at sea, REM sleep often results in sleep paralysis.

<u>EEG: Electrode Placement</u>

For 11 of 13 EEG animals, we measured cranial tissue thickness using ultrasound (2.1 ± 0.2 cm between skin and skull surface). Prior to the experiments, we determined electrode placement based on measurements from postmortem tissues of seals that had died from natural causes unrelated to the study. Measurements of weanling, juvenile, and adult northern elephant seals revealed lowest skull thickness (~3 mm [weanlings]; ~6 mm [juveniles]; ~10 mm [adult females]) above the fronto-parietal region of the brain. In this location, skin thickness in postmortem specimens was ~2 mm [weanlings] to ~12 mm [adult females] and blubber thickness was ~10-15 mm [min-max for weanlings] to ~15-35 mm [min-max for adult females]. A layer of muscle (~5 mm) overlaid the skull below the blubber.

EEG Animal Observations

In addition to the datalogger's inertial motion sensors, we recorded behavior using video cameras whenever possible. Continuous low-resolution webcam footage (Wyze Cam Outdoor 1080p HD Webcam; Wyze Labs, Inc.) and intermittent high-resolution DSLR footage (Nikon® D7200) was used to document fine-scale eye, nostril, and vibrissae movement for seals at Long Marine Lab and while animals were on the beach at Año Nuevo State Park. One weanling elephant seal was instrumented with a small animal-borne camera to observe conspecific interactions. Video data were visually scored at 1 Hz, where we recorded the animal's activity level (galumphing [active forward movement on land], swimming, quiet waking, visibly breathing, or not visibly breathing), posture (prone, supine, left, right, vertical up, or vertical down), social interactions (alone, not alone [conspecifics within 5 m], or social [actively interacting with other animals]), location (land, wet [in water shallower than body height], at surface, or underwater). With high-resolution video, we recorded eye state (open, closed, eye movements), muscle twitches, whisker twitches, and vocalizations.

EEG Data Processing

Binary 500Hz electrophysiological data were converted into EDF (European Data Format) using a custom MATLAB (MathWorks, Inc.) application (Neurologger Converter & Visualizer © Evolocus LLC). Raw electrophysiological data were processed using Independent Components Analysis (ICA) in the MATLAB toolbox EEGLAB (v2020.0) to identify and remove heart signals from EEG, EOG, and EMG, as discussed in previous studies (*18, 45, 46*). Raw signals were always maintained for cross-comparison. We bandpass filtered raw signals for visual analysis consistent with previous studies and the standard outlined in the American Academy of Sleep Medicine (AASM) sleep scoring manual as follows: EEG/EOG: 0.3-30 Hz; EMG: 10-100 Hz; ECG: 0.3–75 Hz (*18*). However, this software filter was limited by the built-in hardware bandpass filter of the Neurologger3 from 1-500 Hz, which adjusts the ultimate filtering for EEG/EOG to 1-30 Hz and ECG to 1-75 Hz.

EEG Qualitative Analysis: Sleep Scoring

Guidelines for visual sleep scoring followed parameters established for lab-based sleep studies of northern elephant seals and other marine mammals (*20, 21, 24-27, 42-43, 47*). Sleep scoring criteria is as follows, with additional qualitative and quantitative criteria in Kendall-Bar *et al.* 2022 (*18*):

1. Quiet Waking (QW) – low voltage, high-frequency background EEG activity (>50% of 30 s epoch) and accelerometer demonstrating only subtle breathing or motion (i.e. rolling, grooming, or repositioning). **2. Active Waking (AW)** – low voltage, high-frequency background EEG with motion artifacts or accelerometer demonstrating more than subtle breathing or motion (>50% epoch). **3. Slow-wave sleep (SWS)** – high voltage, low-frequency (0.5 - 4 Hz) EEG (>50% epoch). We further subdivided SWS into **deep SWS** (maximal amplitude SWS) and **light SWS** (transitional state, voltage >1.5X QW with sleep spindles and K-complexes). **4. Rapid-eye-movement (REM)** – low-voltage, high-frequency EEG with an increase or change in heart rate variability (HRV) compared to SWS or QW. We conservatively subdivided REM into putative REM (REM1) or certain REM (REM2) based on the extent of HRV. We further expand on the criteria and determination of REM sleep below.

EOG and EMG

Before arriving at EEG and HRV as primary scoring criteria for REM, we first checked for the key features of REM sleep, recorded in most mammalian and bird species, including rapid eye movements in EOG and reduced muscle tone in EMG:

EOG: Although eye blinks often coincided with deflections in EOG, we are doubtful that surface-mounted EOG and EMG electrodes were sensitive enough to detect more subtle eye movements or changes in muscle tone. We examined second-to-second correlation between eye movements in video recordings and EOG and observed only partial detection of eye movements via EOG. Thus, rapid eye movements seem to be present in northern elephant seals. However, neither EOG-detected nor video-detected eye movements occurred within each REM episode (see Fig. S1 for an example where no eye movements were detected). As a result, we did not use EOG-detected or video-detected eye movements to determine sleep state.

EMG: There was often minimal to no detected decrease in muscle tone in EMG between SWS and REM sleep, presumably due to the fact that we could not detect this change using surface electrodes or because the change in muscle tone was small. Unlike in other true seals, we did not notice a postural change wherein seals would extend the head forward or drop their heads during REM sleep. This was most likely due to the large size of elephant seals, whose heads were already resting on the ground during preceding SWS episodes. Therefore, it is likely that changes in muscle tone between SWS and REM sleep are minimal for seals resting on land. In water, the buoyant force acting on the head may reduce the amount of muscle tone variation between SWS and REM sleep as well. Additionally, although EMG (and multi-channel electrical artifacts) detected occasional muscle twitches during REM sleep, these were not unique to REM sleep and were not present in each REM sleep episode. Video recordings and electrical artifacts revealed that episodes of REM sleep were accompanied by vibrissa, head, and limb movements (jerks), although the phasic components of REM sleep in elephant seals are less pronounced compared to some other mammalian species (e.g., repeated twitches in the sloth (*48*), continuous eye movements in the mouse deer (*49*) or the periods of intense vibrissae movements in the walrus (*26*)). As a result, we did not rely on EMG to determine sleep state.

We provide EOG and EMG recordings alongside EEG and HRV traces in Fig. S1 to demonstrate the challenges associated with employing surface-mounted EOG and EMG to inform sleep stage characterization for northern elephant seals.

REM Sleep Scoring

We based our scoring of REM sleep using HRV on previous studies of bilateral aquatic sleep in marine mammals (*26*) and further assess the extent of low-frequency HRV by qualitatively assessing the heart rate (HR; bpm) pattern and calculating the variance of the very low frequency (VLF; 0-0.005Hz) power of HR. We scored certain REM2 when this quantitative measure of variance in HRV was high (if VLF power transiently exceeded ~2 (with some interindividual variability)) and putative REM1 when this measure was lower (Fig. S1, S2). REM1 and REM2 were only scored during apnea and between periods of SWS and waking (*42, 43*). During REM1 and REM2, video footage demonstrated behavior consistent with REM, where we observed closed eyes with occasional lid movements, no intentional movement, occasional whisker and muscle twitches, and whole-body jerks. The degree of HRV often varied during an episode of REM sleep. We are inclined to view this as an alternation of phasic (certain REM2) and tonic (putative REM1) periods within one interrupted episode of REM sleep, as described in other mammals (e.g., fur seal, harp seal, walrus; *24-26)*. Eye movements and

twitches were often observed in conjunction with a period of higher heart rate variability, potentially representing a phasic period. We provide sleep scoring results with and without putative REM for comparison (Table S3). The main text presents statistics for cumulative REM (certain and putative REM).

EEG Quantitative Analysis: Spectral Power

We calculated delta spectral power (0.5-4Hz) for EEG channels over 30 s epochs, and very low-frequency (VLF) heart rate (HR) power between 0-0.005 Hz in re-sampled (500Hz matching electrophysiological frequency) automated peak-detected heart rate traces (using the 'large dog' preset in LabChart®; ADInstruments; Colorado, USA). Spectral power analyses were performed with a Fast Fourier Transform (FFT) using a Hann (cosine-bell) data window with 50% overlap at 1K (EEG) or 8K (HRV) resolution. Quantitative analyses of variance of VLF HR Power (Fig. S2) and EEG spectral power confirmed elevated HRV during visually scored REM and elevated delta EEG Power during SWS (Fig. S1, S2).

Signal Quality Analysis

During some recordings, ambient electrical noise created by lab equipment and VHF or satellite transmitters resulted in temporary loss of scorable signals (< 3% of total recording time; Table S2). Nonetheless, we quantified signal quality across full recordings (using δ SWS / δ REM) and recorded at least two-fold greater amplitude SWS signals as compared to REM, despite signal reduction in water (Fig. S3; *18*). It is possible that, at least in part, the reduction in the size of slow waves could represent an adaptive response for increased vigilance in water as is reported in frigatebirds while flying (*10*). However, the decrease in relative SWS amplitude between land and water is most likely the result of decreased signal due to saltwater bridging between electrodes. Methods and validation for this signal quality analysis can be found in Kendall-Bar *et al. 2022* (*18*). Any difference between EEG amplitude across the two hemispheres (as seen in Fig. 1 & S1) was constant over the recording duration for each animal, likely due to differences in electrode impedance, perhaps due to hair growth or local tissue thickness. To analyze interhemispheric asymmetry, we normalized spectral power in each hemisphere during SWS to levels recorded during a neighboring QW episode to account for changes in signal amplitude across hemispheres and across time (as animals transitioned in and out of water). Across 23 sleep bouts (periods of consecutive sleeping dives) in 3 seals at sea, asymmetry between hemispheres with higher and lower delta spectral power did not exceed 2-fold ((δ SWS higher / δ SWS lower)/ δ QW = 0.77 [mean] ± 0.22 [SD]; max = 1.29). Across all seals and recordings, neither quantitative analysis nor visual inspection revealed interhemispheric EEG asymmetry (<2-fold difference) between symmetrical derivations, consistent with 3 prior studies of sleep in true seals *(22)*.

Motion & Environmental Sensor Processing

For EEG studies, inertial motion sensing data was calibrated and processed using the Customized Animal Tracking Systems (CATS) toolbox (*50*). Speed was estimated using a custom MATLAB script based on stroke rate, pitch, and vertical speed using established thresholds for land and aquatic velocity from previous studies (*23, 51*). Processed inertial sensing data and speed estimates were paired with GPS coordinates from Argos transmitters to create dead-reckoned tracks and reconstruct three-dimensional diving patterns. Three-dimensional tracks were then visualized in ArcGIS Pro (© 2019 ESRI) and Maya (© 2022 Autodesk) using

the *Visualizing Life in the Deep* tools and scripts for visualizing underwater behavior (*52, 53*) (Fig. 1, Movie S1).

SWS and REM at sea

We paired separately processed motion and sleep state data to examine the biomechanics of sleep at sea. In this section, we combine values for all SWS (light sleep SWS1 and deep sleep SWS2) and all REM (certain REM1 and putative REM2). On the continental shelf, seals slept while approaching the ocean floor or on the ocean floor (vertical speed ($|d'(t)|$) < 0.1 m/s). Out of 8.11 h of sleep across all seals (N=3) at the continental shelf (78.2% SWS and 21.8% REM), 7.37 h (90.8%) occurred on the ocean floor (76.3% SWS and 23.7% REM). While on the continental shelf, seals were upside down (|roll| > 2 radians) 64.4% of REM time and only 37.0% of SWS time.

In the open ocean, seals slept while drifting in the water column, often entering "sleep spirals" which we defined as at least two consecutive loops in the same direction – clockwise or counterclockwise. Out of 6.16 h of sleep across all seals (N=3) in the open ocean (73.9% SWS and 26.1% REM), 2.65 h (43%) occurred within a sleep spiral (53.8% SWS and 46.2% REM). 76.3% of REM in the open ocean occurred within sleep spirals, but only 31.3% of SWS. This value increases to 81.3% if REM that precedes or follows a sleep spiral is included (if a sleep spiral occurs within the dive but does not overlap with the period of REM in question). The remaining 4 episodes of REM that did not co-occur with a sleep spiral were short with only a single loop and therefore did not meet our definition of a sleep spiral.

Regardless of sleep spiral overlap, seals in the open ocean were upside down for 100% of REM sleep time in 21 REM sleep episodes compared to only 37.3% of SWS time. This supine inversion was also observed in biomechanical studies of juvenile northern elephant seals (N=6; *23*) and adult southern elephant seals (N=12; *54*). A few hypotheses have attempted to explain supine inversions in seals: (a) improved visual detection [of prey] (*23, 55*), (b) slowing descent rate *(23)*, and (c) thicker ventral versus dorsal blubber layers *(23)*. (a) Based on the presence of sleeping EEG activity and absence of foraging behavior during drift dives *(39)*, it is unlikely that seals are maintaining vigilance for prey, but it is possible that the supine posture provides a vigilance benefit for seals occasionally opening their eyes to monitor for predators attacking from below during sleep. However, seals in pools in the lab also often slept in a supine posture. (b) Our data support the fact that this inverted posture coincides with a reduced vertical speed (0.18 ± 0.058 m/s during REM; 0.28 ± 0.15 m/s during SWS).

We cannot conclusively show why seals undergo this supine inversion; we propose that the transition to REM sleep is accompanied by the loss of muscle tone, as in other mammals, at which point the inherent density distribution and shape of the instrumented animal may cause it to passively invert. Captive seals without instrumentation also slept in supine postures. The prevalence of supine inversion during REM sleep as opposed to SWS supports a passive mechanism triggered by REM sleep onset (and not reversed or prohibited by SWS onset- as seen in Fig. 1) as opposed to an active, vigilance-based preference for a supine sleeping posture.

Sleep Identification Model

Data from the EEG logger identify SWS and REM sleep during (A) inactivity on the ocean floor on the continental shelf, (B) inactivity approaching the ocean floor near the continental shelf, (C) inactivity during gliding, usually preceding sleep spirals, (D) inactivity during sleep spirals. While the vertical speed (rate of depth change; $d'(t)$) signatures of SWS and

REM sleep are not distinct (there is some overlap; Fig. S5), we employed the collective signatures of SWS and REM sleep to distinguish potential sleep from non-sleep using a hierarchical filtering algorithm to identify low-vertical-speed segments of time-depth records that likely represent inactivity (Fig. S6). Cases A-D represent four specific types of "drifts" (low-vertical-speed segments) that likely represent sleep based on our EEG data.

We estimated sleep in time-depth records using our EEG results and a hierarchical filtering algorithm to identify potential sleep. The sleep identification model incorporated elements of previously established hierarchical methods for identifying "drift dives," where the first derivative is constant for most of the dive (*30, 37*, *56*). Existing methods often prioritized obtaining smooth estimates of these constant drift rates, used as a proxy for fat content and mass gain via buoyancy (*37*). As such, these methods often rely on data abstraction that reduces complexity (via segmentation or the "broken-stick method") that may not allow for multiple independent drift segments in a single dive (*56*, *57*). This model aimed to assess more sensitively the upper bound of time spent passively drifting through the water column.

Importantly, we refined our sleep identification algorithm to include dives that contained sleep, but that lack the sudden changes in vertical speed typically used to identify drift dives (*56, 57*). These dives, though providing electrophysiological benefits of sleep, would not have been included in previous drift-dive identifications. In addition, current depth-based dive categorization does not differentiate between transiting or resting flat-bottom dives. In our case, benthic sleep accounted for up to 5.2 h per day in an animal sleeping near shore. We incorporated the potential for benthic sleep in our model.

Model implementation

We estimated sleep quotas for N=334 adult female northern elephant seals across foraging trips at sea (N=170 short trips [74.6 ± 9.5 days] and N=164 long trips [217.7 ± 24.7 days]; Table S1). A subset of 14 seals (8 short trips and 6 long trips) were instrumented with accelerometers to assess the false positive rate of our model (propensity to falsely identify segments where the animal is swimming).

We analyzed diving behavior using a custom script in MATLAB that identifies consecutive segments that meet thresholds. Therefore, an important first processing step was to standardize the resolution and sensitivity of each time-depth record. We down-sampled data to 8 s and applied a first pass Gaussian smoother (window size of 6) to remove noise in sensor data. For example, precise depth sensors like the EEG logger's Keller Druck 4LD sensor detected oscillations when the animal rolled back and forth on the seafloor. Smoothing dampens the amplitude of such oscillations. We then rounded the data to the nearest meter to reduce the probability of the first derivative to change sign (which would interrupt a consecutive drift segment). We then smoothed the data again (same window) to obtain consecutive drifts within first derivative thresholds.

To apply an in-situ depth calibration, we applied a zero-offset correction to adjust surface intervals (and associated dives) to zero across the recording. A threshold of 2 meters differentiated surface intervals and dives. A threshold of 15 strokes per minute differentiated periods of stroking and gliding (see explanation above). Glides exceeding 3 minutes (duration that minimized false positives) were labeled long glides.

Extended surface intervals exceeding 10 minutes were included in our sleep estimate, where animals could spend up to 8 hours at the surface without stroking activity. Although we do not have direct EEG observations at sea to confirm this, one animal in the lab spent several days

sleeping vertically at the surface of the pool; such "bottling" is a common sleep behavior for seals and walruses (*25-26*).

To identify drifts, we found consecutive segments satisfying broad preliminary vertical speed and acceleration criteria, compared to existing drift dive identification metrics, to minimize false negatives. These broad vertical speed and acceleration criteria were as follows with $d(t)$ = depth as a function of time: $|d'(t)| < 0.60$ & $|d''(t)| < 0.05$) (Fig. S5, S6). We then applied a minimum duration (>3 min) to identify long drifts. Within long drifts, we kept all long flats as a proxy for benthic sleep in our sleep estimate. Long flats included all long drifts ending in a flat segment ($|\text{mean}(d'(t_{end}))| < 0.01$ m/s where t_{end} is between 7/8 and 8/9 of the segment).

We filtered the remaining long drifts that did not fit the criteria for long flats using the following filter criteria. The filter criteria were designed to maximize accuracy while minimizing false negatives based on EEG data and false positives based on stroking data. Long drifts were maintained as an upper bound sleep estimate to ensure sensitivity in the case of overly sensitive filter criteria. Filter criteria were designed to ensure accuracy and sensitivity across a broad range of challenging scenarios: (i) when animals are positively buoyant while shallow and negative while deep and (ii) when animals are close to neutrally buoyant and drift downwards and upwards in a single dive. Filter criteria minimized false positives (ensured specificity) during: (iii) transit dives (where animals' vertical speed is minimal, but they are actively swimming), and (iv) benthic dives that follow a bottom contour within the vertical speed and acceleration criteria.

First, we eliminated long drifts that deviated from a smoothed drift rate throughout the trip to eliminate physiologically implausible drift rates. We calculated smoothed drift rates for shallow (< 500 m) long drifts using a Gaussian smoother (window size 1/20 of the trip duration). We preserved a broad threshold of drift rates surrounding this smoothed drift rate to minimize false negatives ($|d'(t) - d'(t)_{\text{smoothed}}| < 0.3$ m/s) (Fig. S5, S6). Previous studies implemented similar filters, including spline regressions or Kalman filters (*17*, *39, 57*).

Next, we applied filtered drifts according to the buoyancy of the animal. Generally, the criteria for positively buoyant seals were broader than for negatively buoyant seals. Positively buoyant seals could drift upward and downward, while negatively buoyant seals only drifted downward (Fig. S6). We considered the animal positively buoyant 20 days before this smoothed drift rate exceeded 0 m/s ($t_{positive}$). If an animal was positively buoyant near the beginning of the trip (within the first 20 days), we used the broader positively buoyant criteria for the entire trip.

Filter criteria aimed to minimize false positives by eliminating "benthic travel" (seals swimming along the continental shelf at a relatively constant ascent or descent rate) and "travel" (U-shaped transit dives with low vertical speed) (Fig. S6). Anti-travel criteria eliminated segments where the drift rate changed between the beginning and the end of the drift ($|d'(t_1) - d'(t_2)| < 0.10$ m/s where t_1 is between 1/4 and 2/3 of the segment and t_2 is between 2/3 and 3/4 of the drift duration). Anti-benthic-travel criteria eliminated drifts with slopes lower than 0.08 m/s. For negatively buoyant seals, we only allowed negative long drifts that passed both anti-transit and anti-benthic-travel criteria. For positively buoyant seals, we used different criteria for positive and negative drifts. Positive drifts for positively buoyant seals ($d'(t) > 0$ & $t > t_{positive}$) were eliminated if they violated anti-travel criteria, but not anti-benthic-travel criteria (eliminating curved drifts but not low-slope drifts, because seals near neutral buoyancy could have drift rates near zero). We allowed curved downward drifts for positively buoyant seals, where the seal would be decelerating (Fig. S6). For both positively and negatively buoyant seals, only long negative drifts for positively buoyant seals were kept (> 200s compared to 180s for often-fragmented positive drifts).

For the first and last 15 days from the calculation of smoothed drift rate, where false positives were more likely, we applied more restrictive filtering criteria (0.15 m/s around a drift rate calculated from only the shallow (< 500 m), non-flat long drifts at the beginning or end of the trip). We assumed a constant drift rate calculated based on filtered long drifts for the first and last 15 days. If seals were positively buoyant, we did not restrict drift rates.

The output of these filtering steps, filtered long drifts, were added to long flats (benthic sleep) and extended surface intervals (potential sleep at surface) to constitute our sleep estimate. This sleep estimate represents Total Sleep Time (SWS and REM binned together). Unfiltered long drifts (includes long flats), derived solely from first and second derivative criteria, were added to extended surface intervals to constitute our upper bound sleep estimate.

Accuracy of Sleep Identification

We validated our model by calculating its accuracy ((True Positives [TP] + True Negatives [TN])/All Classifications [TP+TN+FP+FN]), sensitivity (TP/(TP+FN)), and specificity (TN/(FP+TN)) compared to EEG-identified sleep. The sleep identification model yielded 93% accuracy (Fig. 3 & Fig. S7). We also calculated an upper-bound sleep estimate (unfiltered "long drifts") with high sensitivity (93.6%) to minimize false negatives (1.3% of classifications). Simply imposing a duration threshold increased accuracy of our sleep identifier from 46.3% to 77.1%. Our filtering criteria (see previous page and Fig. S6) improved the accuracy of our sleep identification model to 93% overall and decreased false positives from 21.6% to 5.2% (Fig. S7). While the sensitivity of the model decreased from 98.4% to 84.8% (from drifts to filtered long drifts/sleep estimate), the specificity increased from 42.0% to 94.1%. Long glides were fairly accurate (86.3%) and specific (89.9%) to estimate total sleep time, but not as accurate as our sleep identification model. Therefore, we used long glides as a proxy for sleep to identify false positive rates for the 14 adult females instrumented with stroke rate loggers.

We also manually reviewed dive records with the model output for 7 24-h excerpts from different portions of the trip (1%, 20%, 40%, 50%, 60%, 80%, and 99% of trip duration). We rejected diving records where depth sensors malfunctioned.

Spatial Sleep Analysis

All seals were tracked using the Argos system (https://www.argos-system.org/). Erroneous locations on land were first filtered out by cross-referencing to bathymetry data (dataset ID usgsCeSS111). Location estimates were further refined using the foieGras package version 0.7-7.9276 in R (*58-60*), which uses a continuous time state-space model to filter tracking data using Argos location error estimates. Locations were interpolated to match the 10 s diving data and then averaged to obtain mean daily positions. Daily activity and mean positions were plotted, transformed into a raster layer (using 'Kriging' 2D interpolation method and then clipped with 'Extract by Mask' with land cover data (World Land Cover ESA 2009) and clipped to the extent of tracking data (1 point per seal day) to visualize daily sleep estimation across space.

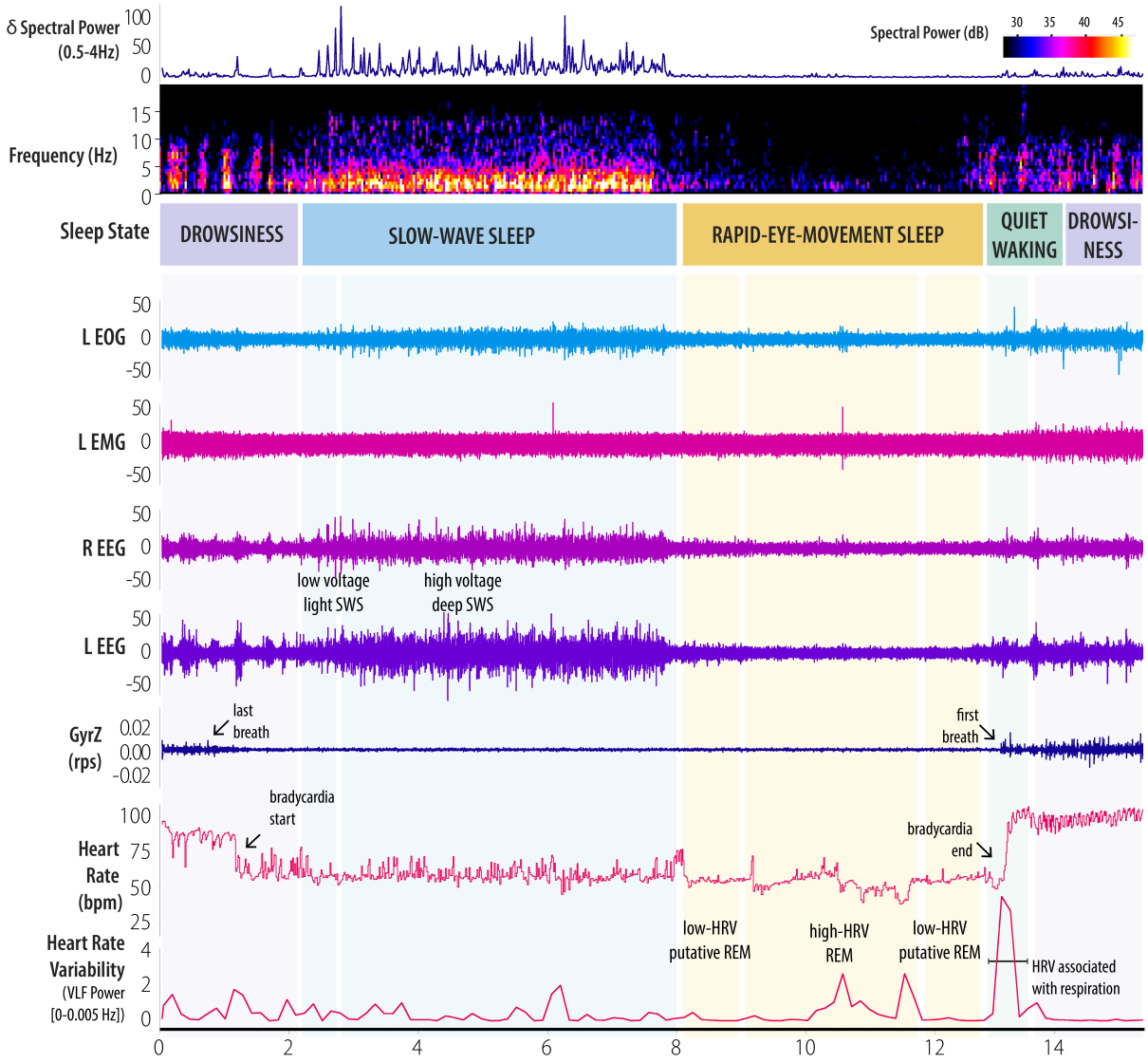

Fig. S1.

Sleep scoring methods. Example 15-minute sleep polygraph of sleep on land demonstrating signals during each sleep stage. Sleep stages were distinguished on the basis of distinct characteristics of the EEG spectrogram (left hemisphere), z-axis gyroscope (for breath detection), and heart rate. Spectral power (left hemisphere) varied across stages from **(1) Drowsiness (DW)** with slow (10 s) oscillations between slow waves and waking, **(2) Slow-Wave Sleep (light SWS: low-amplitude SWS & deep SWS: high-amplitude SWS)** high amplitude low-frequency activity, **(3) REM Sleep** with lowest amplitude high-frequency activity and highest heart rate variability (HRV) **(putative REM: low HRV & certain REM (high HRV))**, and **(4) Quiet Waking (QW)** low amplitude high-frequency activity. To categorize REM sleep, we used the combination of low delta spectral power, apnea [not breathing], and high heart rate variability (not associated transitions from or to eupnea [breathing consistently]). We include EOG and EMG recordings to demonstrate the lack of notable characteristics (no detected eye movements or changes in muscle tone – See "EOG & EMG" above).

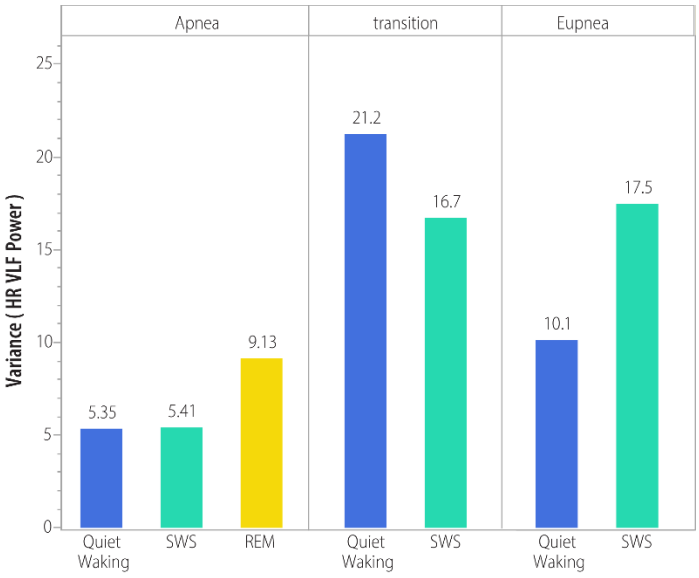

Fig. S2.

Heart rate variability across sleep states. Variance of very low frequency (VLF; 0-0.005 Hz) power for heart rate, sampled once per 10 s. REM has high low-frequency variability compared to SWS and QW during apnea and QW has elevated variability during eupnea and transitions to and from eupnea.

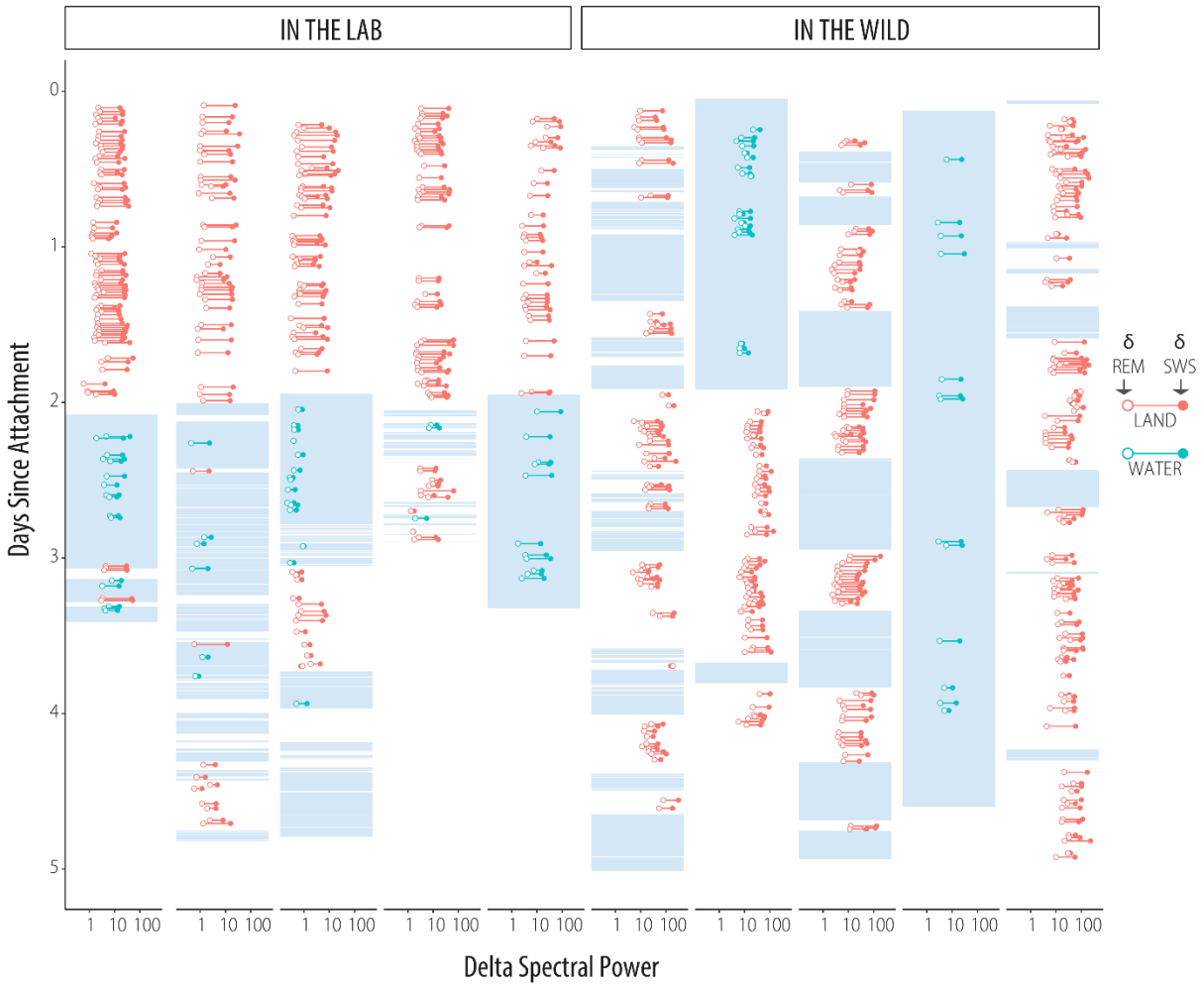

Fig. S3.

Signal quality (δ SWS / δ REM) for 5 recordings in the lab and in the wild. Blue boxes denote submersion in water (in the lab [pool] or in the wild [shallow lagoon or at sea]). Detected signal amplitude during slow wave sleep was smaller during submersion in water, but remained at least 2-fold greater than that during REM.

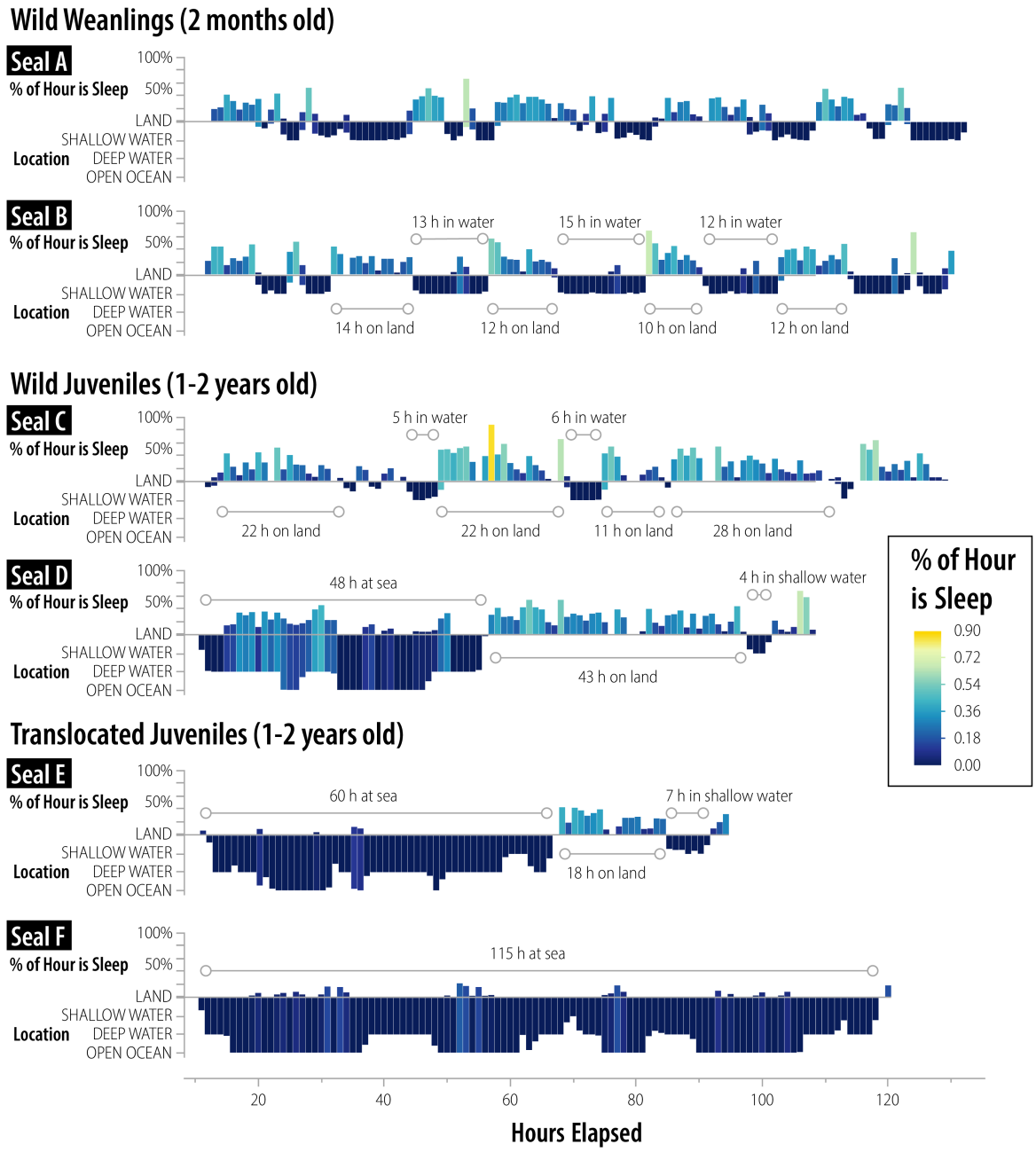

Fig. S4.

Sleep rebound for 6 wild seals. Sleep and location data from EEG recordings for 6 seals (2 wild weanlings [2 months old], 2 wild juveniles [1-2 years old], and 2 translocated juveniles [1-2 years old]). Colors and bars above the x-axis represent the percent of the hour that contained sleep (0-100%). Bars below the x-axis represent the location (Land, Shallow Water, Deep Water, Open Ocean: partial values represent time shared in two habitats). The figure demonstrates that the sleep rebound after 48 h (Seal 4) and 60 h (Seal 5) at sea results in 43 h and 18 h of sleep recovery of similar intensity and duration to the similar-aged wild juvenile that did not leave the breeding colony (Seal 3).

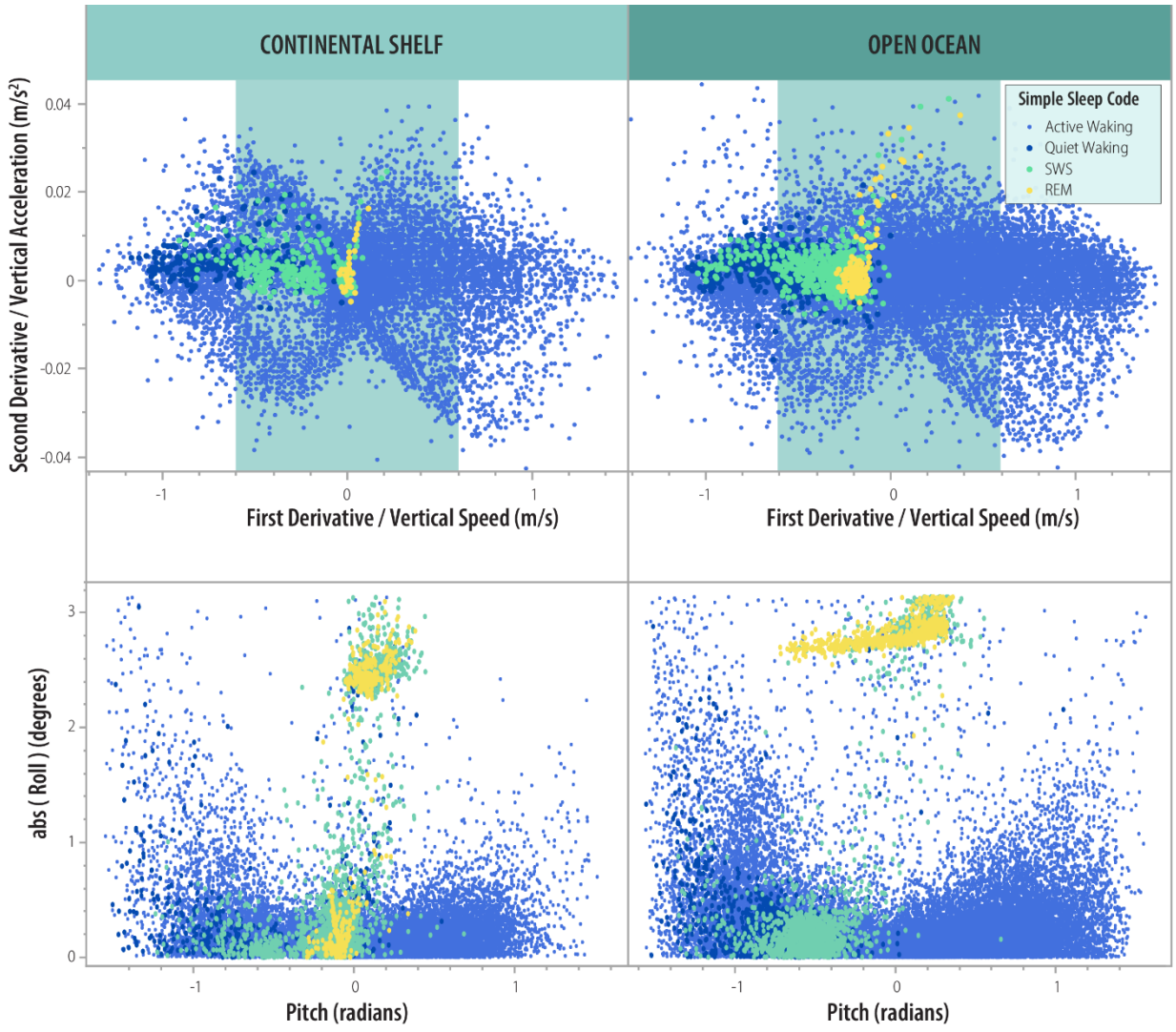

Fig. S5.

Time-depth and three-dimensional correlates of electrophysiological sleep. Quantitative parameters for raw data (at 10 s) by sleep stage (Active Waking [small light blue dots], Quiet Waking [large dark blue dots], SWS [large green dots], and REM [large yellow dots]). Teal rectangle demonstrates first and second derivative thresholds applied to dataset for sleep identification. Note that REM sleep only occurs while animals are rolled upside down, at which point the seals oscillate from pitch up to pitch down.

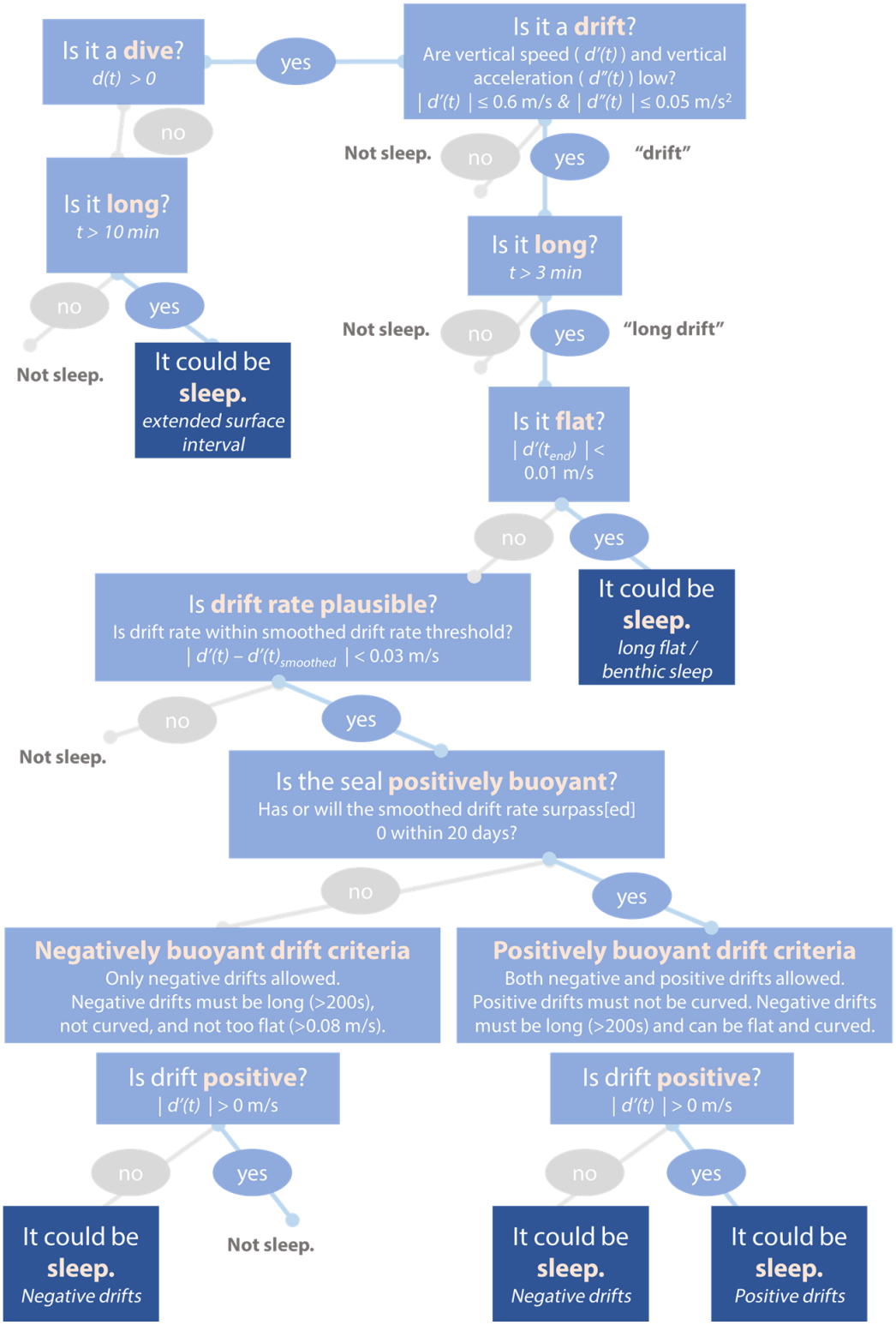

Fig. S6.

Tree diagram for sleep identification model. Tree diagram explaining filtering criteria and the order applied to identify potential sleep episodes.

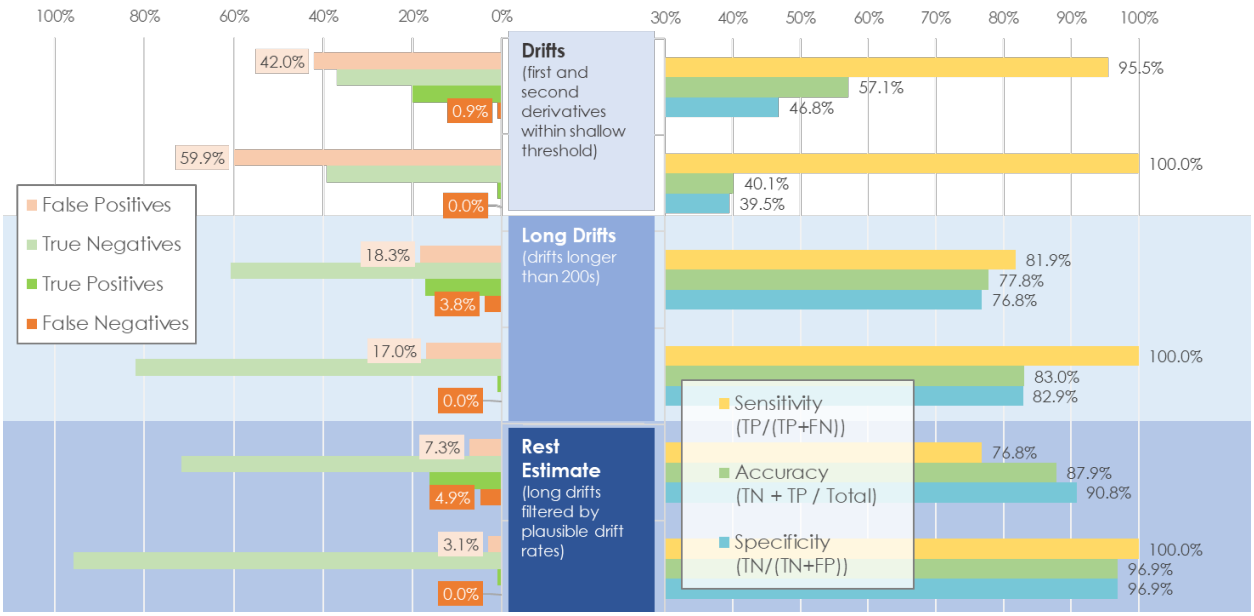

Fig. S7.

Accuracy of sleep identification model for two seals at sea (upper seal slept more than lower seal). Accuracy and specificity increase while the sensitivity and prevalence of false positives decrease from identified drifts to long drifts (longer than 200 s) and finally our filtered sleep estimate (long drifts filtered by plausible drift rate).

Table S1.

	Animal Info.			*Morphometrics*					*Recording duration (days)*					*Data Collected*								
Dataset	**Age Class**	**Sex**	**Age (mo.)**	**Length (cm)**	**Girth (cm)**	**Mass (kg)**	**Location**	**Recording Type**	**Land (LD)**	**Shallow Water (SW)**	**Continental Shelf (CS)**	**Open Ocean (OO)**	**Total Duration (days)**	**EEG**	**ECG**	**Continuous Webcam**	**Animal-borne camera**	**Kami kami**	**3D Motion**	**Stroke Rate**	**High-resolution Video**	**TDR**
EEG Dataset	**Yearling**	**F**	**~8**	152	132	118	LML	Lab	2.1	1.2	0.0	0.0	3.3				-	-				
	Weanling	**F**	**2**	165	143	200	ANO	Wild	0.7	1.8	0.0	0.0	2.6			-		-				
	Juvenile	**F**	**26**	187	102	~120	ANO	Wild	1.8	1.1	0.0	0.0	2.9			-	-	-				
	Juvenile	**F**	**20**	188	124	141	LML	Lab	2.8	1.8	0.0	0.0	4.6				-	-				
	Juvenile	**F**	**20**	206	147	196	LML	Lab	3.1	1.7	0.0	0.0	4.8				-	-				
	Juvenile	**F**	**20**	206	129	177	LML	Lab	2.7	0.2	0.0	0.0	2.9				-	-				
	Yearling	**F**	**~8**	165	139	148	LML	Lab	1.9	1.4	0.0	0.0	3.3				-	-				
	Weanling	**F**	**2**	157	130	116	ANO	Wild	3.0	2.1	0.0	0.0	5.0			-	-	-				
	Juvenile	**F**	**~26**	151	129	118	ANO	Wild	2.1	0.2	1.1	0.7	4.1			-	-	-				
	Weanling	**F**	**2**	177	134	154	ANO	Wild	2.5	2.5	0.0	0.0	5.0			-	-	-				
	Juvenile	**F**	**~26**	177	140	163	XLOC	XLOC	0.3	0.2	1.8	2.5	4.8			-	-	-				
	Juvenile	**F**	**~14**	170	140	157	ANO	Wild	4.2	0.6	0.0	0.0	4.8			-	-	-				
	Juvenile	**F**	**~26**	199	160	211	XLOC	XLOC	1.0	0.5	1.4	0.6	3.5			-	-	-				

	EEG Dataset				*N*	*Type*					*total dur. (d)*	*Data Collected*									
					5	**Lab**	12.6	6.3	0.0	0.0	18.9										
					6	**Wild**	14.3	8.3	1.1	0.7	24.4										
					2	**XLOC**	1.3	0.6	3.2	3.1	8.3										
					13	**Total**	28.2	15.2	4.3	3.9	51.6										

																	Kami kami	**3D Motion**	**Stroke Rate**	**Video**	**TDR**
Time-Depth Record Dataset (TDR)					*N*	*Season*					*mean dur. (d)*	*Data Collected*									
	Adult	**F**			170	**PB**					74.6 ± 9.5										
	Adult	**F**			164	**PM**					217.7 ± 24.7										
Stroke Rate data (SR: subset of TDR Dataset)					*N*	*Season*						*Data Collected*									
	Adult	**F**			8	**PB**															
	Adult	**F**			6	**PM**															

Morphometrics and recording duration for all instrumented seals (electroencephalogram [EEG], time-depth records [TDR], and Stroke Rate [SR] recordings) in this study. For EEG Dataset animals, the table provides age, sex, morphometrics (length [cm], girth [cm], mass [kg]), and recording location (Long Marine Lab [LML], Año Nuevo State Park [ANO], Translocation [XLOC]), recording type (lab, wild, translocation, post-breeding [PB], or post-molt [PM]), recording duration (in days; Land [LD], Shallow Water [SW], Continental Shelf [CS], Open Ocean [OO]), total sleep time (hours per day), and type of data collected (electroencephalogram [EEG], electrocardiogram [ECG], webcam, animal-borne camera, kami-kami [jaw-mounted accelerometer], 3D motion, stroke rate [back or flipper mounted accelerometer], DSLR video, and time-depth recorder).

Table S2.

	Animal Information				*Sleep time summary (total hours)*															
TOPPID	**Age Class**	**Sex**	**Age (mo.)**	**Recording Type**	Active Waking		Quiet Waking		Putative REM Sleep		Certain REM Sleep		LV Slow Wave Sleep		HV Slow Wave Sleep		Drowsiness		Unscorable		Total Scored	Total hours not scored
2019058	**Yearling**	**F**	**~8**	Lab	37.2		11.8		2.9		5.9		5.9		10.1		6.3		1.8		80.1	1.8
2020045	**Weanling**	**F**	**2**	Wild	46.0		3.1		0.6		1.9		3.4		6.5		0.0		12.3		61.5	12.3
2020046	**Juvenile**	**F**	**26**	Wild	52.6		6.4		0.5		1.8		3.3		5.2		0.5		4.7		70.4	4.7
2020047	**Juvenile**	**F**	**20**	Lab	53.4		14.2		1.9		7.5		10.4		16.4		7.3		5.9		111.0	5.9
2020048	**Juvenile**	**F**	**20**	Lab	51.6		16.5		1.6		9.5		10.3		18.4		6.6		1.3		114.6	1.3
2020049	**Juvenile**	**F**	**20**	Lab	29.6		16.2		1.8		6.3		4.1		10.8		0.8		0.1		69.5	0.1
2020050	**Yearling**	**F**	**~8**	Lab	36.8		6.8		1.9		6.2		8.1		18.3		0.6		1.0		78.8	1.0
2021041	**Weanling**	**F**	**2**	Wild	83.1		5.7		1.3		6.9		7.2		16.7		0.1		0.0		120.9	0.0
2021042	**Juvenile**	**F**	**~26**	Wild	53.3		6.4		0.6		7.5		12.4		17.0		1.6		0.0		98.8	0.0
2021043	**Weanling**	**F**	**2**	Wild	73.7		9.0		1.0		9.1		9.2		17.0		0.0		1.1		119.0	1.1
2021044	**Juvenile**	**F**	**~26**	XLOC	109.2		1.4		0.2		1.0		0.7		1.8		0.0		0.0		114.4	0.0
2021045	**Juvenile**	**F**	**~14**	Wild	56.4		10.2		0.7		9.5		13.5		23.2		1.5		4.2		115.0	4.2
2022033	**Juvenile**	**F**	**~26**	XLOC	69.2		4.4		0.3		2.3		3.0		4.8		0.2		2.3		84.1	2.3
					x̄	SD	x̄	SD	x̄	SD	x̄	SD	x̄	SD	x̄	SD	x̄	SD	x̄		SUM	SUM
				Lab	41.7	± 9.2	13.1	± 3.6	2.0	± 0.4	7.1	± 1.3	7.8	± 2.5	14.8	± 3.6	4.3	± 3.0	2.0	± 2.0	453.9	10.0
				Wild	60.8	± 13.1	6.8	± 2.3	0.8	± 0.3	6.1	± 3.1	8.2	± 4.0	14.3	± 6.4	0.6	± 0.7	3.7	± 4.3	585.6	22.4
				XLOC	89.2	± 20.0	2.9	± 1.5	0.3	± 0.0	1.7	± 0.6	1.9	± 1.1	3.3	± 1.5	0.1	± 0.1	1.1	± 1.1	198.6	2.3
				Total	57.9	± 20.7	8.6	± 4.7	1.2	± 0.8	5.8	± 2.9	7.0	± 3.8	12.8	± 6.4	2.0	± 2.7	2.7	± 3.4	1238.1	34.6

Sleep scoring data summary. Total recording time (hours) spent in each sleep stage per recording for each EEG-instrumented seal in this study. Metadata match Table S1. Sleep and wake stages include active waking, quiet waking, putative rapid-eye-movement (REM) sleep, certain REM sleep, low-voltage (LV) slow-wave sleep, high-voltage (HV) slow-wave sleep, and drowsiness. The number of hours of unscorable data are provided for reference.

Table S3.

						24 * (Sleep / Total Scored)	24 * (Sleep / Total Scored)	24 * (Sleep / Total Scored)	24 * (All REM / Total Scored)	24 * (All REM / Total Scored)	24 * (Certain REM / Total Scored)	Certain REM / Total Sleep	All REM / Total Sleep
Animal Information													
Age Class	**Sex**	**Age (mo.)**	**Recording Type**	**Total sleep (h)** (SWS + REM)	Total Scored	**Total Sleep Time [TST] (h/day)** (Sleep = All SWS + All REM)	**TST with Drowsiness (h/day)** (Sleep = All SWS + All REM + Drowsiness)	**TST Certain REM Only (h/day)** (Sleep = All SWS + Certain REM)	**Daily All SWS (h/day)** (All SWS = Light [LV] SWS + Deep [HV] SWS)	**Daily All REM (h/day)** (All REM = Certain REM + Putative REM)	**Daily Certain REM (h/day)** (Certain REM only)	**Certain REM % of TST** (Certain REM only)	**All REM % of TST** (Certain & Putative)
Yearling	**F**	**~8**	Lab	24.8	80.1	7.4	9.3	6.4	4.7	2.6	1.7	23.8%	35.4%
Weanling	**F**	**2**	Wild	12.4	61.5	4.8	4.8	3.8	3.2	0.8	0.6	15.4%	20.2%
Juvenile	**F**	**26**	Wild	10.9	70.4	3.7	3.9	3.3	2.7	0.8	0.6	16.8%	21.8%
Juvenile	**F**	**20**	Lab	36.2	111.0	7.8	9.4	7.0	5.5	1.9	1.5	20.9%	26.0%
Juvenile	**F**	**20**	Lab	39.9	114.6	8.4	9.7	7.9	5.9	2.3	2.0	23.9%	28.0%
Juvenile	**F**	**20**	Lab	22.9	69.5	7.9	8.2	7.3	5.1	2.8	2.2	27.4%	35.2%
Yearling	**F**	**~8**	Lab	34.5	78.8	**10.5**	10.7	9.8	7.9	2.5	1.9	18.1%	23.6%
Weanling	**F**	**2**	Wild	32.1	120.9	6.4	6.4	6.1	4.7	1.6	1.4	21.4%	25.6%
Juvenile	**F**	**~26**	Wild	37.5	98.8	9.1	9.5	9.0	7.1	2.0	1.8	20.1%	21.6%
Weanling	**F**	**2**	Wild	36.3	119.0	7.3	7.3	7.1	5.2	2.0	1.8	25.2%	27.8%
Juvenile	**F**	**~26**	XLOC	3.8	114.4	**0.8**	0.8	0.8	0.5	0.3	0.2	27.0%	33.3%
Juvenile	**F**	**~14**	Wild	46.8	115.0	9.8	10.1	9.3	7.4	2.0	1.9	20.2%	21.6%
Juvenile	**F**	**~26**	XLOC	10.3	84.1	2.9	3.0	2.8	2.2	0.7	0.6	22.0%	24.8%
				x̄	SUM	x̄ ± SD	x̄ ± SD	x̄ ± SD	x̄ ± SD	x̄ ± SD	x̄ ± SD	x̄ ± SD	x̄ ± SD
			Lab	158.3	453.9	8.4 ± 1.1	9.5 ± 0.8	7.7 ± 1.2	5.8 ± 1.1	2.4 ± 0.3	1.9 ± 0.2	22.8% ± 3.1%	29.6% ± 4.8%
			Wild	176.1	585.6	6.9 ± 2.2	7.0 ± 2.3	6.4 ± 2.3	5.1 ± 1.8	1.5 ± 0.5	1.4 ± 0.6	19.9% ± 3.2%	23.1% ± 2.7%
			XLOC	14.1	198.6	1.9 ± 1.1	1.9 ± 1.1	1.8 ± 1.0	1.3 ± 0.8	0.5 ± 0.2	0.4 ± 0.2	24.5% ± 2.5%	29.1% ± 4.3%
			Total	348.5	1238.1	6.7 ± 2.7	7.2 ± 3.0	6.2 ± 2.6	4.8 ± 2.1	1.7 ± 0.8	1.4 ± 0.6	21.7% ± 3.6%	26.5% ± 5.0%

Total sleep time summary table. Total sleep time (TST) calculated with and without putative REM and drowsiness for the 13 seals in our EEG dataset. Metadata match Table S1. This table uses data provided in Table S2 to calculate **TST** (24*(All SWS + All REM)/Total Scored), **TST with Drowsiness** (24*(All SWS + All REM + Drowsiness)/Total Scored), **TST with Certain REM Only** (24*(All SWS + Certain REM)/Total Scored). We also provide the daily hour values for **All SWS** (Low-Voltage [LV] SWS + High-

Voltage [HV] SWS), **All REM** (Certain REM + Putative REM), and **Certain REM**. We compare the proportion of REM/TST (REM % TST) with and without segments scored as putative REM (less pronounced heart-rate variability) for comparison (**Certain REM % of TST** vs. **All REM % of TST**). At the bottom of the table, means and standard deviations are provided for each experimental group (Lab, Wild, Translocation [XLOC], and Total [all EEG animals]).

Table S4.

				TST = (Sleep [All SWS + All REM]) / Total Scored [per Location]										24 * (Sleep / Total Scored)	
Animal Information				***Total Sleep Time (h/day) by Location***											
Age Class	**Sex**	**Age (mo.)**	**Recording Type**	**Land**	**Shallow Water**	**Continental Shelf**	**Open Ocean**	**Max sleep (in 24h)**	**Min sleep (in 24h)**	**Total Sleep Time [TST] (h/day)** (Sleep = All SWS + All REM)	
Yearling	**F**	**~8**	Lab	8.9	4.9	-	-	9.0	5.9	7.4	
Weanling	**F**	**2**	Wild	10.5	2.6	-	-	5.7	3.6	4.8	
Juvenile	**F**	**26**	Wild	5.3	1.3	-	-	3.5	3.1	3.7	
Juvenile	**F**	**20**	Lab	9.7	4.8	-	-	11.6	4.5	7.8	
Juvenile	**F**	**20**	Lab	9.9	5.7	-	-	9.3	6.3	8.4	
Juvenile	**F**	**20**	Lab	8.0	7.2	-	-	7.0	6.9	7.9	
Yearling	**F**	**~8**	Lab	12.6	7.6	-	-	**14.1**	6.8	**10.5**	
Weanling	**F**	**2**	Wild	10.7	0.1	-	-	9.3	4.0	6.4	
Juvenile	**F**	**~26**	Wild	13.0	0.0	7.5	2.6	13.9	5.3	9.1	
Weanling	**F**	**2**	Wild	14.0	0.6	-	-	8.1	6.4	7.3	
Juvenile	**F**	**~26**	XLOC	0.6	0.0	0.0	1.4	1.3	0.6	**0.8**	
Juvenile	**F**	**~14**	Wild	11.1	0.0	-	-	12.6	6.5	9.8	
Juvenile	**F**	**~26**	XLOC	9.6	0.0	0.0	1.0	8.7	**0.0**	2.9	
				x̄ SD	x̄ SD	x̄ SD	x̄ SD	x̄	x̄	x̄ SD	
			Lab	9.8 ± 1.7	6.0 ± 1.3	- ± -	- ± -	14.1	4.5	8.4 ± 1.1	
			Wild	10.8 ± 3.0	0.8 ± 1.0	- ± -	- ± -	13.9	6.5	6.9 ± 2.2	
			XLOC	5.1 ± 6.3	0.0 ± 0.0	0.0 0.0	1.2 ± 0.3	8.7	0.0	1.9 ± 1.1	
			Total	9.5 ± 3.4	2.7 ± 2.8	2.5 ± 3.5	1.7 ± 0.7	14.1	0.0	6.7 ± 2.7	
TDR Dataset			***Season***	*N*						*TST*	
Adult	**F**		**PB**	170						1.1 ± 1.1	
Adult	**F**		**PM**	164						2.2 ± 1.6	

Total sleep time summary table. Total sleep time (TST = Sleep [All SWS + All REM] / Total Scored) in hours per day per recording location for 13 EEG seals in this study. Metadata matches Table S1. TST values are provided for Land, Shallow Water (depth < 10 m), Continental Shelf (depth < 250 m), and the Open Ocean (depth > 250 m). The maximum and minimum sleep times per 24 h period are provided for comparison (max 14.1 h/day and min 0.0 h/day). Mean (x̄) and standard deviation (SD) summarize TST values across

Lab, Wild, Translocation (XLOC), and all animals. Overall TST is provided for all EEG dataset seals alongside sleep estimates derived for adult females in the TDR dataset (bottom of table).

Table S5.

Predicted Class	True Class	True Negatives	False Negatives	False Positives	True Positives	True Negatives (% of total)	False Negatives (% of total)	False Positives (% of total)	True Positives (% of total)	Accuracy (TN + TP / Total)	Sensitivity (TP/(TP+FN))	Specificity (TN/(TN+FP))
		7965	203	9044	4326	37.0%	0.9%	42.0%	20.1%	57.1%	95.5%	46.8%
		18565	7	28128	1621	38.4%	0.0%	58.2%	3.4%	41.8%	99.6%	39.8%
Drifts	Sleep	10533	0	16110	268	39.1%	0.0%	59.9%	1.0%	40.1%	100.0%	39.5%
		37063	**210**	**53282**	**6215**	**38.2%**	**0.3%**	**53.4%**	**8.1%**	**46.3%**	**98.4%**	**42.0%**
		13058	822	3951	3707	60.6%	3.8%	18.3%	17.2%	77.8%	81.9%	76.8%
		32470	18	14223	1610	67.2%	0.0%	29.4%	3.3%	70.5%	98.9%	69.5%
Long Drifts	Sleep	22081	0	4562	268	82.1%	0.0%	17.0%	1.0%	83.0%	100.0%	82.9%
		67609	**840**	**22736**	**5585**	**70.0%**	**1.3%**	**21.6%**	**7.2%**	**77.1%**	**93.6%**	**76.4%**
		15445	1049	1564	3480	71.7%	4.9%	7.3%	16.2%	87.9%	76.8%	90.8%
		44196	365	2497	1263	91.5%	0.8%	5.2%	2.6%	94.1%	77.6%	94.7%
Filtered Long Drifts	Sleep	25819	0	824	268	95.9%	0.0%	3.1%	1.0%	96.9%	100.0%	96.9%
		85460	**1414**	**4885**	**5011**	**86.4%**	**1.9%**	**5.2%**	**6.6%**	**93.0%**	**84.8%**	**94.1%**
		11144	53	5865	4476	51.7%	0.2%	27.2%	20.8%	72.5%	98.8%	65.5%
		37590	18	9103	1610	77.8%	0.0%	18.8%	3.3%	81.1%	98.9%	80.5%
Glides	Sleep	7089	0	19554	268	26.3%	0.0%	72.7%	1.0%	27.3%	100.0%	26.6%
		55823	**71**	**34522**	**6354**	**52.0%**	**0.1%**	**39.6%**	**8.4%**	**60.3%**	**99.2%**	**57.5%**
		15086	328	1923	4201	70.0%	1.5%	8.9%	19.5%	89.5%	92.8%	88.7%
		45794	374	899	1254	94.8%	0.8%	1.9%	2.6%	97.4%	77.0%	98.1%
Long Glides	Sleep	19069	0	7574	268	70.9%	0.0%	28.1%	1.0%	71.9%	100.0%	71.6%
		79949	**702**	**10396**	**5723**	**78.6%**	**0.8%**	**13.0%**	**7.7%**	**86.3%**	**89.9%**	**86.1%**

Performance of sleep identification model. We demonstrate the model's accuracy for identifying sleep using drifts (mathematical first and second derivative criteria alone), long drifts (derivative criteria and time threshold [>3 min]), and filtered long drift (long drifts filtered by criteria explained in Fig. S6). # of categorized samples (8 s^{-1}) that were true negatives (TN – not sleep and not detected), false negatives (FN – sleep but not detected), false positives (FP – not sleep but detected), and true positives (TP – sleep and detected). We show the percentage of total classifications for each category and provide measures of model accuracy (TN + TP / Total), sensitivity (TP / (TP + FN)), and specificity (TN / (TN + FP)).

Movie S1.

Data-driven animation of sleep spiral behavior. Rectangular prisms represent data for each second of a 23-minute dive, colored according to sleep state (Active Waking: blue; Quiet Waking: light blue; Slow Wave Sleep: green; Rapid-eye-movement Sleep: yellow) and rotated according to the animal's pitch, roll, and heading. The seal's swimming behavior is data-generated using peak-detection of the z-axis gyroscope. Additional data shown include stroke rate over time (in strokes per minute [spm]), the EEG spectrogram showing power across frequency over time, depth [m], heart rate [bpm], and minutes into the dive. Screenshot of animation provided below.

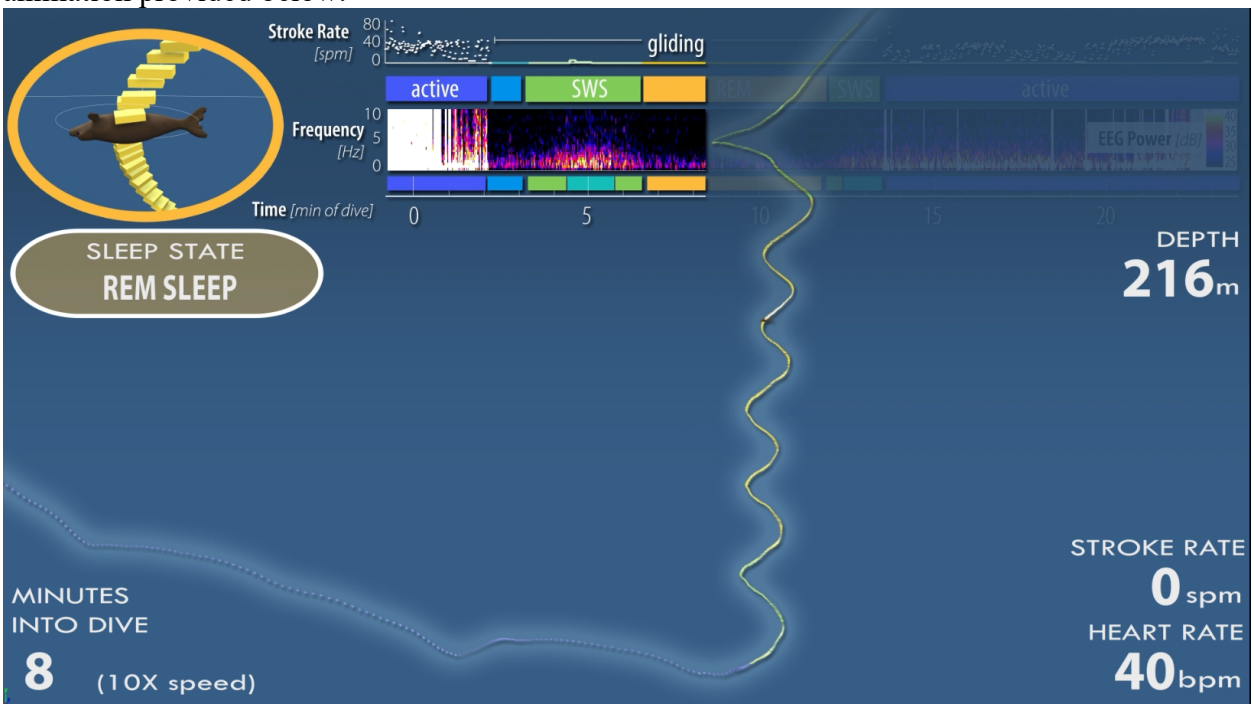

References and Notes

1. J. M. Siegel, Clues to the functions of mammalian sleep. *Nature* **437**, 1264–1271 (2005). doi:10.1038/nature04285 Medline

2. C. V. Senaratna, J. L. Perret, C. J. Lodge, A. J. Lowe, B. E. Campbell, M. C. Matheson, G. S. Hamilton, S. C. Dharmage, Prevalence of obstructive sleep apnea in the general population: A systematic review. *Sleep Med. Rev.* **34**, 70–81 (2017). doi:10.1016/j.smrv.2016.07.002 Medline

3. C. M. Almeida, A. Malheiro, Sleep, immunity and shift workers: A review. *Sleep Sci.* **9**, 164–168 (2016). doi:10.1016/j.slsci.2016.10.007 Medline

4. C. A. Wyse, A. N. Coogan, C. Selman, D. G. Hazlerigg, J. R. Speakman, Association between mammalian lifespan and circadian free-running period: The circadian resonance hypothesis revisited. *Biol. Lett.* **6**, 696–698 (2010). doi:10.1098/rsbl.2010.0152 Medline

5. J. A. Lesku, N. C. Rattenborg, M. Valcu, A. L. Vyssotski, S. Kuhn, F. Kuemmeth, W. Heidrich, B. Kempenaers, Adaptive sleep loss in polygynous pectoral sandpipers. *Science* **337**, 1654–1658 (2012). doi:10.1126/science.1220939 Medline

6. N. C. Rattenborg, S. L. Lima, C. J. Amlaner, Half-awake to the risk of predation. *Nature* **397**, 397–398 (1999). doi:10.1038/17037 Medline

7. E. Ternman, L. Hänninen, M. Pastell, S. Agenäs, P. P. Nielsen, Sleep in dairy cows recorded with a non-invasive EEG technique. *Appl. Anim. Behav. Sci.* **140**, 25–32 (2012). doi:10.1016/j.applanim.2012.05.005

8. T. Belling, Sleep patterns in the horse. *Equine Practice* **12**, 2–26 (1990).

9. J. A. Lesku, L. C. R. Meyer, A. Fuller, S. K. Maloney, G. Dell'Omo, A. L. Vyssotski, N. C. Rattenborg, Ostriches sleep like platypuses. *PLOS ONE* **6**, e23203 (2011). doi:10.1371/journal.pone.0023203 Medline

10. N. C. Rattenborg, B. Voirin, S. M. Cruz, R. Tisdale, G. Dell'Omo, H.-P. Lipp, M. Wikelski, A. L. Vyssotski, Evidence that birds sleep in mid-flight. *Nat. Commun.* **7**, 12468 (2016). doi:10.1038/ncomms12468 Medline

11. O. I. Lyamin, P. R. Manger, S. H. Ridgway, L. M. Mukhametov, J. M. Siegel, Cetacean sleep: An unusual form of mammalian sleep. *Neurosci. Biobehav. Rev.* **32**, 1451–1484 (2008). doi:10.1016/j.neubiorev.2008.05.023 Medline

12. R. A. Martin, N. Hammerschlag, Marine predator-prey contests: Ambush and speed versus vigilance and agility. *Mar. Biol. Res.* **8**, 90–94 (2012). doi:10.1080/17451000.2011.614255

13. M. J. Weise, D. P. Costa, Total body oxygen stores and physiological diving capacity of California sea lions as a function of sex and age. *J. Exp. Biol.* **210**, 278–289 (2007). doi:10.1242/jeb.02643 Medline

14. S. J. Jorgensen, S. Anderson, F. Ferretti, J. R. Tietz, T. Chapple, P. Kanive, R. W. Bradley, J. H. Moxley, B. A. Block, Killer whales redistribute white shark foraging pressure on seals. *Sci. Rep.* **9**, 6153 (2019). doi:10.1038/s41598-019-39356-2 Medline

15. P. W. Robinson, D. P. Costa, D. E. Crocker, J. P. Gallo-Reynoso, C. D. Champagne, M. A. Fowler, C. Goetsch, K. T. Goetz, J. L. Hassrick, L. A. Hückstädt, C. E. Kuhn, J. L.

Maresh, S. M. Maxwell, B. I. McDonald, S. H. Peterson, S. E. Simmons, N. M. Teutschel, S. Villegas-Amtmann, K. Yoda, Foraging behavior and success of a mesopelagic predator in the northeast Pacific Ocean: Insights from a data-rich species, the northern elephant seal. *PLOS ONE* **7**, e36728 (2012). doi:10.1371/journal.pone.0036728 Medline

16. N. Hammerschlag, R. A. Martin, C. Fallows, Effects of environmental conditions on predator–prey interactions between white sharks (*Carcharodon carcharias*) and Cape fur seals (*Arctocephalus pusillus pusillus)* at Seal Island, South Africa. *Environ. Biol. Fishes* **76**, 341–350 (2006). doi:10.1007/s10641-006-9038-z

17. T. Adachi, A. Takahashi, D. P. Costa, P. W. Robinson, L. A. Hückstädt, S. H. Peterson, R. R. Holser, R. S. Beltran, T. R. Keates, Y. Naito, Forced into an ecological corner: Round-the-clock deep foraging on small prey by elephant seals. *Sci. Adv.* **7**, eabg3628 (2021). doi:10.1126/sciadv.abg3628 Medline

18. J. M. Kendall-Bar, R. Mukherji, J. Nichols, C. Lopez, D. A. Lozano, J. K. Pitman, R. R. Holser, R. S. Beltran, M. Schalles, C. L. Field, S. P. Johnson, A. L. Vyssotski, D. P. Costa, T. M. Williams, Eavesdropping on the brain at sea: Development of a surface-mounted system to detect weak electrophysiological signals from wild animals. *Anim. Biotelem.* **10**, 16 (2022). doi:10.1186/s40317-022-00287-x

19. N. C. Rattenborg, C. J. Amlaner, S. L. Lima, Behavioral, neurophysiological and evolutionary perspectives on unihemispheric sleep. *Neurosci. Biobehav. Rev.* **24**, 817–842 (2000). doi:10.1016/S0149-7634(00)00039-7 Medline

20. J. M. Kendall-Bar, A. L. Vyssotski, L. M. Mukhametov, J. M. Siegel, O. I. Lyamin, Eye state asymmetry during aquatic unihemispheric slow wave sleep in northern fur seals (*Callorhinus ursinus*). *PLOS ONE* **14**, e0217025 (2019). doi:10.1371/journal.pone.0217025 Medline

21. O. I. Lyamin, L. M. Mukhametov, J. M. Siegel, E. A. Nazarenko, I. G. Polyakova, O. V. Shpak, Unihemispheric slow wave sleep and the state of the eyes in a white whale. *Behav. Brain Res.* **129**, 125–129 (2002). doi:10.1016/S0166-4328(01)00346-1 Medline

22. O. I. Lyamin, J. M. Siegel, Sleep in aquatic mammals. *Handb. Behav. Neurosci.* **30**, 375–393 (2019). doi:10.1016/B978-0-12-813743-7.00025-6 Medline

23. Y. Mitani, R. D. Andrews, K. Sato, A. Kato, Y. Naito, D. P. Costa, Three-dimensional resting behaviour of northern elephant seals: Drifting like a falling leaf. *Biol. Lett.* **6**, 163–166 (2010). doi:10.1098/rsbl.2009.0719 Medline

24. O. I. Lyamin, P. O. Kosenko, S. M. Korneva, A. L. Vyssotski, L. M. Mukhametov, J. M. Siegel, Fur seals suppress REM sleep for very long periods without subsequent rebound. *Curr. Biol.* **28**, 2000–2005.e2 (2018). doi:10.1016/j.cub.2018.05.022 Medline

25. O. I. Lyamin, Sleep in the harp seal (*Pagophilus groenlandica*). Comparison of sleep on land and in water. *J. Sleep Res.* **2**, 170–174 (1993). doi:10.1111/j.1365-2869.1993.tb00082.x Medline

26. O. I. Lyamin, P. O. Kosenko, A. L. Vyssotski, J. L. Lapierre, J. M. Siegel, L. M. Mukhametov, Study of sleep in a walrus. *Dokl. Biol. Sci.* **444**, 188–191 (2012). Medline

27. O. I. Lyamin, P. O. Kosenko, J. L. Lapierre, L. M. Mukhametov, J. M. Siegel, Fur seals display a strong drive for bilateral slow-wave sleep while on land. *J. Neurosci.* **28**, 12614–12621 (2008). doi:10.1523/JNEUROSCI.2306-08.2008 Medline

28. B. J. Le Boeuf, D. E. Crocker, "Diving behavior of elephant seals: Implications for predator avoidance," in *Great White Sharks, The Biology of* Carcharodon carcharias, A. P. Klimley and D. G. Ainley, Eds. (Academic Press, 1996), pp. 193–205.

29. D. E. Crocker, B. J. L. Boeuf, D. P. Costa, Drift diving in female northern elephant seals: Implications for food processing. *Can. J. Zool.* **75**, 27–39 (1997). doi:10.1139/z97-004

30. Y. Naito, D. P. Costa, T. Adachi, P. W. Robinson, M. Fowler, A. Takahashi, Unravelling the mysteries of a mesopelagic diet: A large apex predator specializes on small prey. *Funct. Ecol.* **27**, 710–717 (2013). doi:10.1111/1365-2435.12083

31. R. R. Holser, D. E. Crocker, P. W. Robinson, R. Condit, D. P. Costa, Density-dependent effects on reproductive output in a capital breeding carnivore, the northern elephant seal (*Mirounga angustirostris*). *Proc. Biol. Sci.* **288**, 20211258 (2021). doi:10.1098/rspb.2021.1258 Medline

32. N. Gravett, A. Bhagwandin, R. Sutcliffe, K. Landen, M. J. Chase, O. I. Lyamin, J. M. Siegel, P. R. Manger, Inactivity/sleep in two wild free-roaming African elephant matriarchs - Does large body size make elephants the shortest mammalian sleepers? *PLOS ONE* **12**, e0171903 (2017). doi:10.1371/journal.pone.0171903 Medline

33. Data for: J. M. Kendall-Bar, T. M. Williams, R. Mukherji, D. A. Lozano, J. K. Pitman, R. R. Holser, T. Keates, R. S. Beltran, P. W. Robinson, D. E. Crocker, T. Adachi, O. I. Lyamin, A. L. Vyssotski, D. P. Costa, Brain activity of diving seals reveals short sleep cycles at depth, Dryad (2023); https://doi.org/10.7291/D1ZT2B.

34. Code for: J. M. Kendall-Bar, T. M. Williams, R. Mukherji, D. A. Lozano, J. K. Pitman, R. R. Holser, T. Keates, R. S. Beltran, P. W. Robinson, D. E. Crocker, T. Adachi, O. I. Lyamin, A. L. Vyssotski, D. P. Costa, Brain activity of diving seals reveals short sleep cycles at depth, Zenodo (2023); https://doi.org/10.5281/zenodo.7702650.

35. B. J. Le Boeuf, P. A. Morris, S. B. Blackwell, D. E. Crocker, D. E. Costa, Diving behavior of juvenile northern elephant seals. *Can. J. Zool.* **74**, 1632–1644 (1996). doi:10.1139/z96-181

36. G. W. Oliver, "Homing and diving studies of translocated northern elephant seals," thesis, University of California, Santa Cruz, CA (1997).

37. P. W. Robinson, S. E. Simmons, D. E. Crocker, D. P. Costa, Measurements of foraging success in a highly pelagic marine predator, the northern elephant seal. *J. Anim. Ecol.* **79**, 1146–1156 (2010). doi:10.1111/j.1365-2656.2010.01735.x Medline

38. S. S. Kienle, A. S. Friedlaender, D. E. Crocker, R. S. Mehta, D. P. Costa, Trade-offs between foraging reward and mortality risk drive sex-specific foraging strategies in sexually dimorphic northern elephant seals. *R. Soc. Open Sci.* **9**, 210522 (2022). doi:10.1098/rsos.210522 Medline

39. T. Adachi, J. L. Maresh, P. W. Robinson, S. H. Peterson, D. P. Costa, Y. Naito, Y. Y. Watanabe, A. Takahashi, The foraging benefits of being fat in a highly migratory marine mammal. *Proc. Biol. Sci.* **281**, 20142120 (2014). doi:10.1098/rspb.2014.2120 Medline

40. R. D. Andrews, D. R. Jones, J. D. Williams, P. H. Thorson, G. W. Oliver, D. P. Costa, B. J. Le Boeuf, Heart rates of northern elephant seals diving at sea and resting on the beach. *J. Exp. Biol.* **200**, 2083–2095 (1997). doi:10.1242/jeb.200.15.2083 Medline

41. M. Horning, R. D. Andrews, A. M. Bishop, P. L. Boveng, D. P. Costa, D. E. Crocker, M. Haulena, M. Hindell, A. G. Hindle, R. R. Holser, S. K. Hooker, L. A. Hückstädt, S. Johnson, M.-A. Lea, B. I. McDonald, C. R. McMahon, P. W. Robinson, R. L. Sattler, C. R. Shuert, S. M. Steingass, D. Thompson, P. A. Tuomi, C. L. Williams, J. N. Womble, Best practice recommendations for the use of external telemetry devices on pinnipeds. *Anim. Biotelem.* **7**, 20 (2019). doi:10.1186/s40317-019-0182-6

42. M. A. Castellini, W. K. Milsom, R. J. Berger, D. P. Costa, D. R. Jones, J. M. Castellini, L. D. Rea, S. Bharma, M. Harris, Patterns of respiration and heart rate during wakefulness and sleep in elephant seal pups. *Am. J. Physiol.* **266**, R863–R869 (1994). Medline

43. W. Milsom, M. Castellini, M. Harris, J. Castellini, D. Jones, R. Berger, S. Bahrma, L. Rea, D. Costa, Effects of hypoxia and hypercapnia on patterns of sleep-associated apnea in elephant seal pups. *Am. J. Physiol.* **271**, R1017–R1024 (1996). Medline

44. G. W. Oliver, P. A. Morris, P. H. Thorson, B. J. Le Boeuf, Homing behavior of juvenile northern elephant seals. *Mar. Mamm. Sci.* **14**, 245–256 (1998). doi:10.1111/j.1748-7692.1998.tb00714.x

45. M. D. Schalles, D. S. Houser, J. J. Finneran, P. Tyack, B. Shinn-Cunningham, J. Mulsow, Measuring auditory cortical responses in *Tursiops truncatus*. *J. Comp. Physiol. A Neuroethol. Sens. Neural Behav. Physiol.* **207**, 629–640 (2021). doi:10.1007/s00359-021-01502-5 Medline

46. S. Romero, M. A. Mañanas, S. Clos, S. Gimenez, M. J. Barbanoj, Reduction of EEG artifacts by ICA in different sleep stages. *IEEE.* **3**, 2675–2678 (2003). doi:10.1109/IEMBS.2003.1280467

47. O. I. Lyamin, J. L. Lapierre, P. O. Kosenko, L. M. Mukhametov, J. M. Siegel, Electroencephalogram asymmetry and spectral power during sleep in the northern fur seal. *J. Sleep Res.* **17**, 154–165 (2008). doi:10.1111/j.1365-2869.2008.00639.x Medline

48. B. Voirin, M. F. Scriba, D. Martinez-Gonzalez, A. L. Vyssotski, M. Wikelski, N. C. Rattenborg, Ecology and neurophysiology of sleep in two wild sloth species. *Sleep* **37**, 753–761 (2014). doi:10.5665/sleep.3584 Medline

49. O. I. Lyamin, J. M. Siegel, E. A. Nazarenko, V. V. Rozhnov, Sleep in the lesser mouse-deer (*Tragulus kanchil*). *Sleep* **45**, zsab199 (2022). doi:10.1093/sleep/zsab199 Medline

50. D. E. Cade, W. T. Gough, M. F. Czapanskiy, J. A. Fahlbusch, S. R. Kahane-Rapport, J. M. J. Linsky, R. C. Nichols, W. K. Oestreich, D. M. Wisniewska, A. S. Friedlaender, J. A. Goldbogen, Tools for integrating inertial sensor data with video bio-loggers, including estimation of animal orientation, motion, and position. *Anim. Biotelem.* **9**, 34 (2021). doi:10.1186/s40317-021-00256-w

51. K. A. Tennett, D. P. Costa, A. J. Nicastro, F. E. Fish, Terrestrial locomotion of the northern elephant seal (*Mirounga angustirostris*): Limitation of large aquatically adapted seals on land? *J. Exp. Biol.* **221**, jeb180117 (2018). doi:10.1242/jeb.180117 Medline

52. J. Kendall-Bar, N. Kendall-Bar, A. G. Forbes, G. McDonald, P. J. Ponganis, C. Williams, M. Horning, A. Hindle, H. Klinck, R. S. Beltran, A. S. Friedlaender, D. Wiley, D. P. Costa, T. M. Williams, Visualizing life in the deep: A creative pipeline for data-driven animations to facilitate marine mammal research, outreach, and conservation. *IEEE VIS Arts Program* **2021**, 1 (2021). doi:10.1109/VISAP52981.2021.00007

53. J. Kendall-Bar, "Visualizing life in the deep: Code repository for visualizing marine mammal tag data," GitHub (2021); https://github.com/jmkendallbar/VisualizingLifeintheDeep.

54. K. A. McGovern, D. H. Rodriguez, M. N. Lewis, R. W. Davis, Diving classification and behavior of free-ranging female southern elephant seals based on three-dimensional movements and video-recorded observations. *Mar. Ecol. Prog. Ser.* **620**, 215–232 (2019). doi:10.3354/meps12936

55. M. Kilian, G. Dehnhardt, F. D. Hanke, How harbor seals (*Phoca vitulina*) pursue schooling herring. *Mamm. Biol.* **80**, 385–389 (2015). doi:10.1016/j.mambio.2015.04.004

56. S. A. Gordine, M. Fedak, L. Boehme, Fishing for drifts: Detecting buoyancy changes of a top marine predator using a step-wise filtering method. *J. Exp. Biol.* **218**, 3816–3824 (2015). doi:10.1242/jeb.118109 Medline

57. F. Arce, S. Bestley, M. A. Hindell, C. R. McMahon, S. Wotherspoon, A quantitative, hierarchical approach for detecting drift dives and tracking buoyancy changes in southern elephant seals. *Sci. Rep.* **9**, 8936 (2019). doi:10.1038/s41598-019-44970-1 Medline

58. I. D. Jonsen, C. R. McMahon, T. A. Patterson, M. Auger-Méthé, R. Harcourt, M. A. Hindell, S. Bestley, Movement responses to environment: Fast inference of variation among southern elephant seals with a mixed effects model. *Ecology* **100**, e02566 (2019). doi:10.1002/ecy.2566 Medline

59. I. D. Jonsen, T. A. Patterson, "foieGras: fit latent variable movement models to animal tracking data for location quality control and behavioural inference" (R package Version 0.7-6, (2020).

60. I. D. Jonsen, T. A. Patterson, D. P. Costa, P. D. Doherty, B. J. Godley, W. J. Grecian, C. Guinet, X. Hoenner, S. S. Kienle, P. W. Robinson, S. C. Votier, S. Whiting, M. J. Witt, M. A. Hindell, R. G. Harcourt, C. R. McMahon, A continuous-time state-space model for rapid quality control of argos locations from animal-borne tags. *Mov. Ecol.* **8**, 31 (2020). doi:10.1186/s40462-020-00217-7 Medline